Chinese Chemical Letters 31 (2020) 2721–2724

Contents lists available at ScienceDirect

Chinese Chemical Letters

journal homepage: www.elsevier.com/locate/cclet

Communication

# Visible light-assisted peroxydisulfate activation *via* hollow copper tungstate spheres for removal of antibiotic sulfamethoxazole

Minxian Zhang[a], Jie He[a], Yibo Chen[b,c,**], Pei-Yu Liao[b], Zhao-Qing Liu[b], Mingshan Zhu[a,*]

[a] School of Environment, Jinan University, Guangzhou 510632, China
[b] School of Chemistry and Chemical Engineering, Guangzhou Key Laboratory for Clean Energy and Materials, Guangzhou University, Guangzhou 510006, China
[c] Department of Chemistry, University of California, Riverside, CA 92521, United States

ARTICLE INFO

*Article history:*
Received 14 February 2020
Received in revised form 16 April 2020
Accepted 3 May 2020
Available online 8 May 2020

*Keywords:*
Copper tungstate
Peroxydisulfate
Sulfamethoxazole
Visible light
Hollow spheres

ABSTRACT

The contamination of antibiotics in aqueous environment causes increasing concerns recently. Light-assisted activation of peroxydisulfate (PDS) has been demonstrated as an efficient technology for removal of contamination in water. Herein, a hollow sphere of $CuWO_4$ (h-$CuWO_4$) was employed as a visible light-activated photocatalyst for the activation of PDS, and following with high removal efficiency (98%) of antibiotic sulfamethoxazole (SMX). Under visible light irradiation, the degradation rate on hollow structures system is nearly 2 times higher than the traditional solid $CuWO_4$ spheres. Furthermore, the underlying mechanism and detailed pathway of SMX degradation were proposed based on density functional theory (DFT) calculations and liquid chromatography-mass spectrometry (LC–MS). This work provides a new feasible way for advanced oxidation processes to remove antibiotics SMX in heterogeneous system, and open up new application possibilities of $CuWO_4$-based materials.
© 2020 Chinese Chemical Society and Institute of Materia Medica, Chinese Academy of Medical Sciences. Published by Elsevier B.V. All rights reserved.

Recently, the contamination of the aqueous environment by antibiotics has been observed in various kinds of water and has attracted increasing concerns [1–3]. Sulfamethoxazole (SMX), as a bacteriostatic sulfonamide, is mainly used in the anti-infection treatment of avian cholera to prevent urinary tract infection, respiratory tract infection and intestinal infection [4,5]. Due to the less efficient elimination of SMX in conventional waste water treatment plants, a large portion of SMX is discharged unchanged into the sewage system [6,7]. Therefore, effective methods for removal of SMX from water have become a hot topic.

Advanced oxidation processes (AOPs) based on the peroxydisulfate (PDS), because of their efficient degradation performance and adaptability of the emerging contaminants, have gained increasing attention recently [8–10]. This is because the activation of PDS can generate reactive sulfate radicals ($SO_4^{\bullet-}$), which possess higher redox potential and longer lifetime than hydroxyl radicals ($^{\bullet}OH$) [11,12]. Generally, PDS can be activated by using homogeneous transition metal ions, such as Fe(II), Co(II) or Ag(I), *etc.* [13,14]. However, the discharge of these metal ions into water bodies would lead to serious secondary contamination. Therefore, it is extremely desirable to design novel and well-defined catalysts for the effective activation of PDS.

Photocatalytic technology has attracted extensive attention for removal of organic pollutants, owing to its superior performances such as room temperature operation, solar energy ultization and secondary contamination [15–17]. More recently, combining with photocatalytic techbolgy, light-assisted activation of PDS has been demonstrated as an efficient and green technology for removal of contamination in water [18–23]. Copper tungstate ($CuWO_4$) as a well-known n-type semiconductor which owns narrow band gap (2.2–2.4 eV), is used to be a photocatalyst in various photocatalytic applications [24,25]. On one hand, the property of narrow bandgap semiconductor provides higher ability for conversion of solar energy to chemical energy and then to activate PDS. On the other hand, $CuWO_4$ has abundant architectures, which will show interesting property based on unique structure and open up new application opportunities. For example, we successfully synthesized solid and hollow spheres $CuWO_4$ structures, in which hollow spheres structure has higher adsorption ability for the removal of dyes pollutants [26].

The above attractive results inspire us to take the advantage of the narrow bandgap and unique architecture of $CuWO_4$ to construct a visible-light activated PDS system. Herein, we used

* Corresponding author.
** Corresponding author at: School of Environment, Jinan University, Guangzhou 510632, China.
*E-mail addresses:* chenyibo@gzhu.edu.cn (Y. Chen), zhumingshan@jnu.edu.cn (M. Zhu).

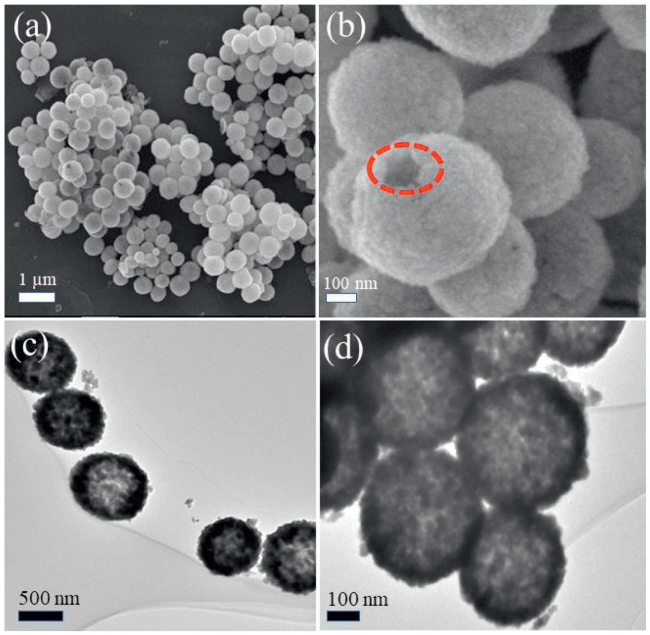


**Fig. 1.** SEM (a and b) and TEM (c and d) images of h-$CuWO_4$ structures.

hollow $CuWO_4$ spheres (h-$CuWO_4$) to activate PDS under visible light illumination, and then the produced radicals triggered the removal of antibiotic SMX. The result shows that the h-$CuWO_4$ exhibits higher removal rate of SMX than solid $CuWO_4$ spheres (s-$CuWO_4$) in the presence of PDS under visible light (VL) irradiation. Electron paramagnetic resonance (EPR) and quenching experiments show that sulfate radical ($SO_4^{\bullet-}$), hydroxyl radicals ($^{\bullet}OH$), singlet oxygen ($^1O_2$) and photo-generated holes contributed to the degradation of SMX in h-$CuWO_4$/PDS/VL system. At the same time, density functional theory (DFT) calculations and liquid chromatography-mass spectrometry (LC–MS) were applied to obtain understanding of the SMX degradation mechanism and pathways.

To reveal the architectures-structures of as-prepared samples, scanning electron microscope (SEM) and transmission electron microscopy (TEM) an images of h-$CuWO_4$ and s-$CuWO_4$ were measured. SEM images of the h-$CuWO_4$ (Figs. 1a and b) show the uniform dispersed grain-like morphology. Moreover, relatively rough and some of the cracks and incomplete parts clearly show the hollow structure of the h-$CuWO_4$. As shown in the Figs. 1c and d, TEM images of h-$CuWO_4$ further confirm the hollow structure. The corresponding SEM and TEM images of s-$CuWO_4$ were shown in Fig. S1 (Supporting information). Besides the basic morphology properties, X-ray diffractometer (XRD) patterns, X-ray photoelectron spectroscopy (XPS) and UV–vis diffuse reflectance spectra of h-$CuWO_4$ and s-$CuWO_4$ were provided in Figs. S2–4 (Supporting information). All the data indicate the successful formation of the $CuWO_4$ samples. The obvious light absorption in visible light range predicts the application possibility of the samples for the activation of PDS to remove the antibiotic pollutants.

Fig. S5 (Supporting information) shows that the PDS alone with/without visible light conditions were hardly degrade SMX, indicating limited efficiency of PDS activation by using pure PDS. To study the photo-assisted PDS activation of h-$CuWO_4$ and s-$CuWO_4$, control experiments using h-$CuWO_4$/PDS, h-$CuWO_4$/VL, h-$CuWO_4$/PDS/VL, and s-$CuWO_4$/PDS, s-$CuWO_4$/VL, s-$CuWO_4$/PDS/VL systems were evaluated and shown in Fig. 2a. First, the adsorption experiments show that less than 2% of SMX are removed by adsorption, which indicates that adsorption isn't the main process for removing SMX. Within 180 min of the reaction, s-$CuWO_4$/VL system had negligible degradation activity, while h-$CuWO_4$/VL system showed that the degradation efficiency of SMX is 8.7%. In the presence of PDS, the degradation efficiencies for s-$CuWO_4$ and h-$CuWO_4$ systems increased to 11% and 15%, respectively. However, under the visible light-assisted activation of PDS, s-$CuWO_4$/PDS/VL system and h-$CuWO_4$/PDS/VL system achieved degradation efficiencies of 80% and 98%, respectively. As shown in Fig. 2b, the observed rate ($k$) of SMX degradation by h-$CuWO_4$/PDS/VL system was 0.022 $min^{-1}$, which is nearly 2 times higher than s-$CuWO_4$/PDS/VL system (0.008 $min^{-1}$). The reason for such increase is due to special hollow structure resulting in the carries' multiple reflection inside the cavity [27], which leading the h-$CuWO_4$ effectively to suppress the recombination rates of photo-induced electron-hole pairs [26]. Compared with the recent reports on light-assisted PDS for removal of pollutants, the optimal h-$CuWO_4$ shows a remarkable catalytic performance (Table S1 in Supporting information).

The effects of h-$CuWO_4$/PDS/VL system about operation parameters on degradation of SMX and h-$CuWO_4$ reproducibility were investigated, and the results were shown in Fig. S6 (Supporting information). Beside the activity, another issue of catalyst is reproducibility. Three cycling experiments of h-$CuWO_4$ for degradation SMX were performed (Fig. S7a in Supporting information). The results showed only slight decrease after three cycles. Moreover, the corresponding XRD pattern of h-$CuWO_4$ (Fig. S7b in Supporting information) further indicated little change for the used h-$CuWO_4$ compared with the fresh one. We also investigated leaching concentration of $Cu^{2+}$ in the residual SMX solution, and only 0.2% of $Cu^{2+}$ is leaching after reaction (Fig. S8 in Supporting information). These results confirmed the good reusability and stability of h-$CuWO_4$.

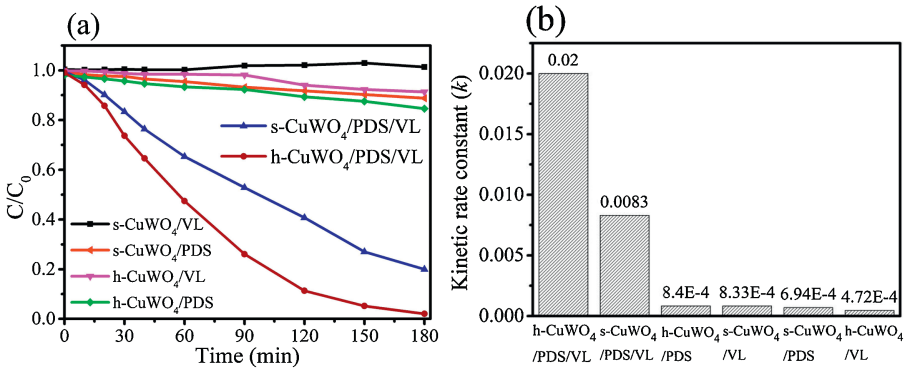


**Fig. 2.** (a) SMX degradation and (b) *pseudo*-first order kinetics of SMX degradation under PDS activation by different materials. Experimental conditions: $[PDS]_0$ = 1.85 mmol/L, $[SMX]_0$ = 10 mg/L, [h-$CuWO_4$] = [s-$CuWO_4$] = 0.375 g/L, pH = 9.0 and T = 25 °C.

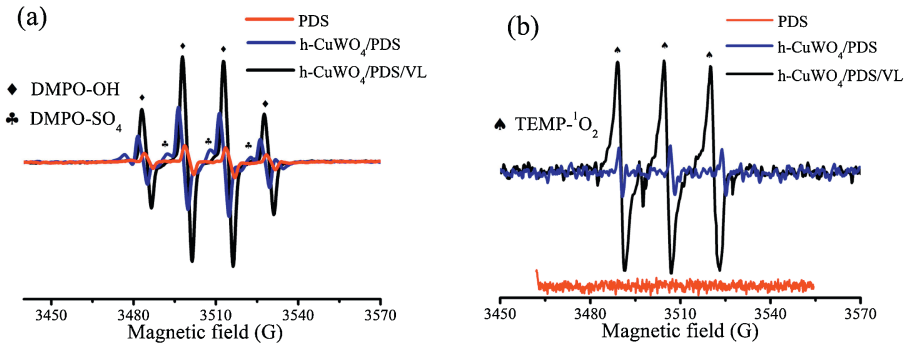


**Fig. 3.** EPR spectra of multiple h-$CuWO_4$/PDS/VL systems. (a) DMPO-OH, DMPO-$SO_4^{\bullet-}$; (b) TEMP-$^1O_2$.

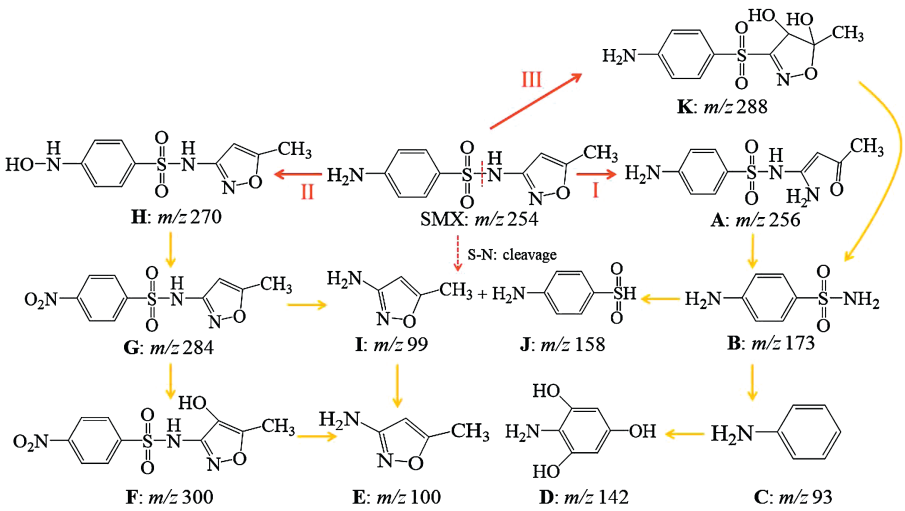


**Fig. 4.** Proposed degradation pathways of SMX in h-$CuWO_4$/PDS/VL system.

In order to investigate the species of radicals in the h-$CuWO_4$/PDS/VL system, different free radical quenchers (*i.e.*, methanol, TBA, KI and FFA) were applied for identifying the primary radical species. The detailed results were shown in Fig. S9 (Supporting information), which indicate that the species of $^{\bullet}OH$, $SO_4^{\bullet-}$, $^1O_2$ radicals and photo-generated holes play synergy actions for the removal of SMX pollutants.

To further confirm the presence of $^{\bullet}OH$, $SO_4^{\bullet-}$ and $^1O_2$ radicals in the h-$CuWO_4$/PDS/VL system, electron paramagnetic resonance (EPR) technique was carried out. In Fig. 3a, both of the h-$CuWO_4$/PDS system and h-$CuWO_4$/PDS/VL system have the characteristic signals of DMPO-OH (four-line signal with the intensities of 1:2:2:1 and special hyperfine coupling constants of $\alpha N = \alpha H = 14.9$ G [28]) and DMPO-$SO_4$, indicating h-$CuWO_4$ can promote the generation of $^{\bullet}OH$ and $SO_4^{\bullet-}$ for the degradation of SMX. Among them, the characteristics $^{\bullet}OH$ and $SO_4^{\bullet-}$ signal peaks of the h-$CuWO_4$/PDS/VL system are stronger than those in the h-$CuWO_4$/PDS system. Fig. 3b shows that the characteristic EPR signals of $^1O_2$ (three lines of equal intensity) are displayed in both the h-$CuWO_4$/PDS system and the h-$CuWO_4$/PDS/VL system, indicating that $^1O_2$ is generated in h-$CuWO_4$/PDS system [29]. Among them, the $^1O_2$ characteristic peak in the h-$CuWO_4$/PDS/VL system is much stronger than that in h-$CuWO_4$/PDS system. The results show that h-$CuWO_4$ can further promote the decomposition of PDS to generate reactive oxygen species (ROS) and degrade SMX under visible light. Therefore, during the decomposition of SMX in the h-$CuWO_4$/PDS combination process, $^{\bullet}OH$, $SO_4^{\bullet-}$ and $^1O_2$ contribute simultaneously.

To further investigate the reaction mechanism, LC–MS and DFT calculations were performed to clarify the products during removal of SMX by h-$CuWO_4$/PDS/VL system [30]. The DFT calculations and Fukui function values were calculated by the Gaussian 09 and details were appended in supporting information. It is generally believed that the larger $f^0$ of the reaction sites, the greater reactivity can be achieved [31,32]. It can be easy to find that 7S ($f^0 = 0.806$), 8 N ($f^0 = 0.306$), 9O ($f^0 = 0.184$) have a large value of $f^0$ (Fig. S10 and Table S2 in Supporting information), which are most possible sites to be attacked by reactive species. And then combined with the intermediates identified by LC–MS, and the

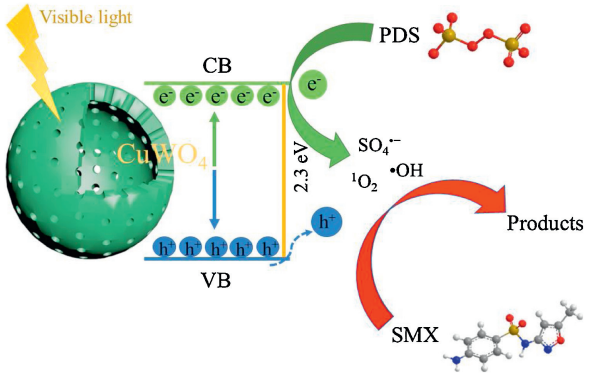


**Fig. 5.** Proposed mechanism of SMX degradation in h-$CuWO_4$/PDS/VL system.

preliminary reaction pathways was proposed in Fig. 4. It could be seen that the highest $f^0$ value of 7S atom was the most susceptible site to be attacked by the radicals and caused the cleavage of S—N and S—C bond adjacent to the S atom. Thus, the S—N bond of SMX can directly fracture and produce product **I** and *J*. In pathway III, radicals attacking on substituted ring can induce the hydroxylation of SMX to form product **K**, and the S—N bond could be attacked by radicals and decomposed to sulfanilamide product **B**. Afterwards, further decomposed into product *J* through oxidized by radicals. Besides, the higher $f^0$ value of 8 N atom suggested that the aniline group was possibly to be oxidized through the radical attacking and resulting in the oxidative formation of product **G** (pathway II). Low molecular weight compounds (*e.g.*, product **E**, **D**, **I**) and ring-open products formed after further deep oxidation of the intermediates. Finally, all small organic fragments were potentially oxidized to $CO_2$ and $H_2O$.

Based on the above results, the proposed mechanism is as following: Electrons and holes could be produced in the h-$CuWO_4$ under visible light because of its narrow band semiconductor structure. Under visible light, the $e^-$ in the valance band (VB) of h-$CuWO_4$ can be excited to its conduction band (CB), and the $h^+$ remains within its VB [33,34]. Because of the carries' confined movement route in the shell [27], h-$CuWO_4$ can effectively suppress the recombination rates of photo-induced electron-hole pairs, promote the charge mobility. Then, these separated charge could react with PDS and water solution to produce ROS ($SO_4^{\bullet-}$, $^{\bullet}OH$, $^1O_2$) [35]. Simultaneously, the generated ROS can rapid decompose SMX to achieve efficient catalytic activity. Based on the above discussion, the detailed reaction mechanisms are illustrated by Fig. 5 and the following formulas (Eqs. 1–8).

$$\text{h-CuWO}_4 + h\nu\ (\lambda > 420\ \text{nm}) \rightarrow \text{h-CuWO}_4\ (e^- + h^+) \quad (1)$$

$$e^- + O_2 \rightarrow O_2^{\bullet-} \quad (2)$$

$$h^+ + H_2O \rightarrow {}^{\bullet}OH + H^+ \quad (3)$$

$$S_2O_8^{2-} + e^- \rightarrow SO_4^{\bullet-} + SO_4^{2-} \quad (4)$$

$$S_2O_8^{2-} + 2H_2O \rightarrow 3SO_4^{2-} + O_2^{\bullet-} + 4H^+ \quad (5)$$

$$SO_4^{\bullet-} + H_2O \rightarrow SO_4^{2-} + {}^{\bullet}OH + H^+ \quad (6)$$

$$SO_4^{\bullet-} + OH^- \rightarrow SO_4^{2-} + {}^{\bullet}OH \quad (7)$$

$$^{\bullet}OH + O_2^{\bullet-} \rightarrow {}^1O_2 + {}^{\bullet}OH \quad (8)$$

In conclusion, PDS activation by h-$CuWO_4$ under the assistance of visible light for high-efficient SMX degradation was observed. The kinetic analysis showed the observed rate of the h-$CuWO_4$/PDS/VL system was 86 times that of h-$CuWO_4$/PDS system without light irradiation and 2 times higher than the traditional s-$CuWO_4$/PDS/VL. Radicals of $SO_4^{\bullet-}$, $^{\bullet}OH$, $^1O_2$ together with photogenerated holes were the dominant active species for the degradation of SMX. Besides, DFT calculation provided insights into the SMX degradation mechanism, which indicated that the 2C, 4C, 6C, 7S, 8 N, 9O atoms were susceptible to be attacked by the oxidative species. Furthermore, the experimental detection of intermediates by MS showed good agreement with the theoretical calculation. This work opens new possibility to develop catalyst for highly efficient degradation of SMX *via* visible light-assisted activation of PDS in heterogeneous system.

## Declaration of competing interest

The authors declare that they have no known competing financial interests or personal relationships that could have appeared to influence the work reported in this paper.

## Acknowledgments

This work was sponsored by the Guangdong Basic and Applied Basic Research Foundation (No. 2020B1515020038). The authors also thank to Prof. Wanqian Guo from Harbin Institute of Technology for DFT calculation.

## Appendix A. Supplementary data

Supplementary material related to this article can be found, in the online version, at doi:https://doi.org/10.1016/j.cclet.2020.05.001.

## References

[1] X. Wang, R. Yin, L. Zeng, M. Zhu, Environ. Pollut. 253 (2019) 100–110.
[2] D. Chen, H. Ngo, W. Guo, et al., J. Hazard. Mater. 387 (2020) 121682.
[3] J. Li, Y. Li, Z. Xiong, W. Guo, B. Lai, Chin. Chem. Lett. 30 (2019) 2139–2146.
[4] C. Wang, Y. Liu, T. Zhou, et al., Chin. Chem. Lett. 30 (2019) 2231–2235.
[5] Y. Zhang, F. Zhao, F. Wang, et al., Chemosphere 246 (2020) 125642.
[6] J. Yan, J. Peng, L. Lai, et al., Environ. Sci. Technol. 52 (2018) 14302–14310.
[7] D. Hu, H. Min, H. Wang, et al., Bioresour. Technol. 52 (2020) 123070.
[8] C. Liu, B. Wu, X.E. Chen, Chem. Eng. J. 335 (2018) 865–875.
[9] S. Waclawek, H.V. Lutze, K. Grübel, et al., Chem. Eng. J. 330 (2017) 44–62.
[10] S. Xiao, M. Cheng, H. Zhong, et al., Chem. Eng. J. 384 (2020) 123265.
[11] X. Duan, H. Sun, S. Wang, Acc. Chem. Res. 51 (2018) 678–687.
[12] X. Chen, W.D. Oh, T.T. Lim, Chem. Eng. J. 354 (2018) 941–976.
[13] G.P. Anipsitakis, D.D. Dionysiou, Appl. Catal. B: Environ. 54 (2004) 155–163.
[14] J. Fernandez, P. Maruthamuthu, J. Kiwi, J. Photochem. Photobiol. A: Chem. 161 (2004) 185–192.
[15] K.Kaur Parul, R. Badru, P.P. Singh, S. Kaushal, J. Environ. Chem. Eng. 8 (2020) 103666.
[16] W. Liu, W. Zhang, M. Liu, et al., Chin. Chem. Lett. 30 (2019) 2177–2180.
[17] P. Chen, Q. Zhang, L. Shen, et al., Chemosphere 216 (2019) 341–351.
[18] R. Yin, Y. Chen, S. He, et al., J. Hazard. Mater. 388 (2020) 121996.
[19] A.H. Mamaghani, F. Haghighat, C.S. Lee, Appl. Catal. B: Environ. 203 (2017) 247–269.
[20] W. Zhu, Z. Li, C. He, S. Faqian, Y. Zhou, J. Alloys Compd. 754 (2018) 153–162.
[21] C. Wang, Y. Liu, T. Zhou, et al., Chin. Chem. Lett. 30 (2019) 2231–2235.
[22] M. Ma, L. Chen, J. Zhao, W. Liu, H. Ji, Chin. Chem. Lett. 30 (2019) 2191–2195.
[23] H. Zhang, J. He, C. Zhai, M. Zhu, Chin. Chem. Lett. 30 (2019) 2338–2342.
[24] F. Duanmu, Z. Shen, Q. Liu, S. Zhong, H. Ji, Chin. Chem. Lett. 31 (2020) 1114–1118.
[25] P. Wang, Z. Shen, Y. Xia, et al., Adv. Funct. Mater. 29 (2019) 1807013.
[26] J. Li, Y. Chen, Z. Wang, Z. Liu, J. Colloid, Interface Sci. 526 (2018) 459–469.
[27] B. Qiu, Q. Zhu, M. Du, et al., Angew. Chem. Int. Ed. 56 (2017) 2684–2688.
[28] J. Cui, L. Zhang, B. Xi, J. Zhang, X. Mao, Chem. Eng. J. 313 (2017) 815–825.
[29] S. Lan, Y. Chen, L. Zeng, et al., J. Hazard. Mater. 393 (2020) 122448.
[30] W. Liu, Y. Li, F. Liu, et al., Water Res. 151 (2019) 8–19.
[31] F. Liu, J. Liang, L. Chen, M. Tong, W. Liu, J. Mol. Liq. 275 (2019) 807–814.
[32] R.G. Parr, W. Yang, J. Am. Chem. Soc. 14 (2002) 4049–4050.
[33] C. Buck, N. Skillen, J. Robertson, P.K.J. Robertson, Chin. Chem. Lett. 29 (2018) 773–777.
[34] Q. Chen, L. Chen, J. Qi, et al., Chin. Chem. Lett. 30 (2019) 1214–1218.
[35] J. Wang, S. Wang, Chem. Eng. J. 334 (2018) 1502–1517.